

Robust Output Regulation for Missile Guidance Against Weaving Targets

Eric D. Peterson*

Technology Service Corporation, Huntsville, AL, 35806

Harry G. Kwatny†

Drexel University, Philadelphia, PA 19104

Proportional navigation is a simple and effective interceptor guidance law. Proportional navigation creates a collision course by regulating the relative Line-of-Sight rates to zero. However, evasive maneuvers may amplify miss distances from knowledge of interceptor vulnerabilities. In addition to evasion, threat maneuver may be intrinsic, such as reentry vehicle oscillation. An interceptor may have approximate knowledge of both physical and evasive threat maneuver dynamics. This paper embeds the maneuver dynamics into the regulator using robust, or structurally stable, regulation. Robustness with respect to error in the embedded maneuver dynamics is characterized and a missile autopilot application is provided.

I. Nomenclature

α, γ, θ	=	{Attack, Flight Path, Pitch} Angle (<i>deg</i>)
q	=	Pitch Rate (<i>deg/s</i>)
δ	=	Fin deflection angle (<i>deg</i>)
M_α, M_δ	=	{Angle of Attack, Fin Deflection} Moment Derivative ($1/s^2$)
Z_α, Z_δ	=	{Angle of Attack, Fin Deflection} Normal Force Derivative ($1/s$)
Q	=	Dynamic Pressure (N/m^2)
x_{ref}, S_{ref}	=	Reference {Length (<i>m</i>), Area (m^2)}
V, V_C	=	{Interceptor, Closing} velocity (<i>m/s</i>)
N'	=	Proportional Navigation Guidance gain
x, ϑ, η	=	{Plant, Exogenous, Error driven controller} state
ω_T, ω_C	=	{Target Manuever, Controller Internal Model} period (<i>rad/s</i>)
Z, Z_C	=	{Exogenous, controller Internal Model} dynamics matrix
n_T, n_L	=	{Target, Interceptor} maneuver acceleration (m/s^2)
A, B, C, D	=	{Dynamic, Input, Output, Feedforward} Plant Matrices

II. Introduction

Proportional navigation (ProNav) guidance has an appealing simplicity and is shown to be optimal in [1] and references. The strengths and weaknesses of ProNav are thoroughly documented in the literature, [2] for example. Maneuvering targets may exploit ProNav weaknesses to evade intercept. Evasive maneuvers informed by approximate interceptor time constant and guidance gain can enlarge miss distances. Interceptor improvements, such as responsiveness (i.e. time constants), may be uneconomic. Guidance improvements include predicting threat maneuvers, estimating maneuver acceleration, or sophisticated nonlinear, hybrid, or differential game strategies. A guidance improvement that

*Engineer, AIAA Member

†S. Herbert Raynes Professor, Department of Mechanical Engineering & Mechanics, AIAA Member

assumes the form of threat maneuver is proposed. The form of evasive maneuvers studied herein are constant frequency weave, where approximate weave frequency is assumed known but neither amplitude nor acceleration is known.

Proportional Navigation regulates to zero the line of sight (LOS) rate ($\dot{\lambda}$). But what effect does threat maneuver have on the LOS rates? And can an approximation of threat maneuver dynamics be exploited to regulate the LOS rate? Regulation that embeds an internal model of exogenous dynamics is called robust regulation [3]. The internal model, required for robustness[4], provides zeros to cancel poles of the threat maneuver dynamics [5]. Performance degradation due to inexact knowledge of threat weave frequency is quantified in Sec. III.B. A performance comparison of robust regulation versus ProNav guidance is illustrated in Sec. III and IV.

Threat maneuvers may be evasive or physical in origin. For example, intrinsic oscillation of re-entry vehicles may effect exo- or high endo-atmospheric intercepts ([2] and sources). An endo-atmospheric, skid-to-turn missile autopilot [6] application of robust regulation with sinusoidal internal model is detailed in Sec. IV. Robust regulator design in Sec. II.C follows [3].

A. Maneuvering Target

Evasive maneuvers considered in this paper take the form

$$\text{target maneuver } n_T = a_T \sin \omega_T t \quad (1)$$

where a_T has units g , e.g. $1g = 9.81 \text{ m/s}^2$, and angular frequency ω_T (rad/sec). Regulator robustness with respect to inaccurate knowledge of ω_T is illustrated in Figs. 3 and 4. In general, robust regulation Eqn. 5 accommodates threat maneuvers of type: step, ramp, sinusoidal, exponential, and linear combinations thereof.

B. Proportional Navigation Guidance Loop

Proportional navigation commands acceleration (n_C) in proportion to the Line of Sight rates ($\dot{\lambda}$)

$$n_C = N' V_C \dot{\lambda} \quad (2)$$

where N' is a guidance gain and V_C is the closing velocity [1]. A collision course along similar triangles is maintained by constant line of sight angles (λ) when line of sight rates are driven to zero. Proportional navigation is computationally simple, robust, and does not require explicit 'time to go' calculation. Fig. 1 is a rudimentary proportional navigation guidance loop with a single, dominate autopilot response time constant τ (sec).

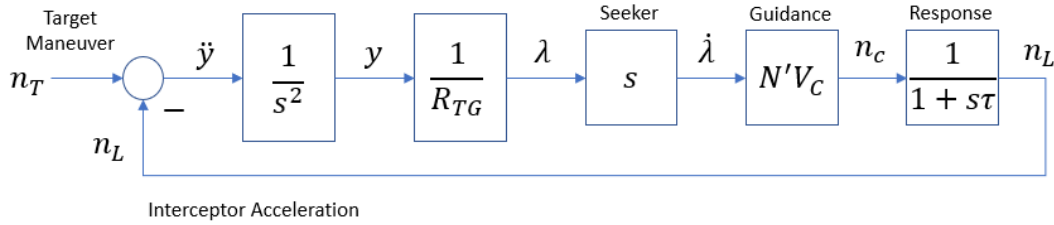


Fig. 1 Proportional Navigation Guidance Loop adapted from [2]

Block diagram reduction of Fig. 1 leads to a linear approximation of the LOS rate equation

$$\dot{\lambda} = \frac{1}{s} \frac{1}{R_{GO}} (n_T - n_L) \quad (3)$$

where R_{GO} is range to go, and s is the Laplace operator. Since threat maneuver n_T is sinusoidal, the LOS rate does not go to zero unless $n_L = n_T$; thereby motivating a controller design with embedded threat maneuver dynamics. The robust regulator formulated below may be applied to intercept and rendezvous.

C. Robust Regulator

Given a Linear Time Invariant (LTI) plant

$$\begin{aligned}\dot{x} &= Ax + Bu \\ y &= Cx + Du\end{aligned}\quad (4)$$

with state vector $x \in R^n$, input $u \in R^m$, and output $y \in R^r$. Append exogenous dynamics and define reference outputs as

$$\begin{aligned}\dot{\vartheta} &= A\vartheta + Bu \\ \dot{\vartheta} &= Z\vartheta \\ e &= F\vartheta - (Cx + Du) = y_{ref} - y\end{aligned}\quad (5)$$

with exogenous dynamic state vector $\vartheta \in R^q$. This paper considers output reference signals such that $F \in R^{m \times q}$ but not exogenous disturbances so $E = 0_{n \times q}$. Controller design follows Synthesis B in [3]. For the error dynamic controller

$$\dot{\eta} = Z\eta + Je \quad (6)$$

choose J such that Eqn. 6 is controllable. Then design a state feedback controller

$$u = -K \begin{bmatrix} x \\ \eta \end{bmatrix}$$

to stabilize

$$\begin{bmatrix} \dot{x} \\ \dot{\eta} \end{bmatrix} = \begin{bmatrix} A & 0 \\ JC & Z \end{bmatrix} \begin{bmatrix} x \\ \eta \end{bmatrix} + \begin{bmatrix} B \\ JD \end{bmatrix} u \quad (7)$$

The Z in Eqns. 6 and 7 is the *internal model* of the exogenous dynamics (ϑ) in Eqn. 5

Regulation $e(t) \rightarrow 0$ is guaranteed *robust* to small variations in plant parameters A , B , C , and D and reference input F . For precise limits on robustness, consider [7]. The objective of this paper is two-fold: 1) apply robust regulation to missile guidance and 2) quantify robustness to perturbations in the internal model Z , specifically the difference between actual and perceived target weave frequency. Performance with respect to inaccurate internal model of weave frequency is compared to proportional navigation in Sec. III.B.

The above regulator design assumes plant states x are known. For this paper, the position and velocity of the interceptor and target dynamics is assumed known. If threat state estimation is needed, observer design is routine [3]. Note that regulation with respect to a sinusoidal reference position output does not require target acceleration, since this is not an (acceleration) augmented form of proportional navigation. Instead, robust regulation works by providing a model of the exogenous dynamics Z of Eqn. 5 inside the controller Eqn. 7.

Observe that Eqn. 6 filters the error signal through a copy of the exogenous dynamics. This internal model of the exogenous dynamics is pictured in Fig. 2 for the SISO output reference case where

$$\phi(s) = (sI_q - Z)$$

and the plant (Eqn. 4) is decomposed into numerator $N(s)$ and denominator $D(s)$ terms. Computing the closed loop transfer function

$$e = y_{ref} - y = \frac{D\phi}{D\phi + N} \cdot \frac{1}{\phi} \vartheta_0 \quad (8)$$

observe the internal copy of the reference input dynamics in the controller produces zeros $\phi(s)$ which cancel poles $\phi(s)$ of the reference input [5], pg. 490.

Note that Eqn. 4 accommodates feedforward terms. Therefore, Condition 4 of Theorem 1 in [3] is modified as

$$\text{rank} \begin{bmatrix} A - \lambda_i & B \\ C & D \end{bmatrix} = n + r, \text{ for each } \lambda_i \text{ in the spectrum of } Z$$

In other words, plant (Eqn. 4) transmission zeros do not cancel the internal model poles.

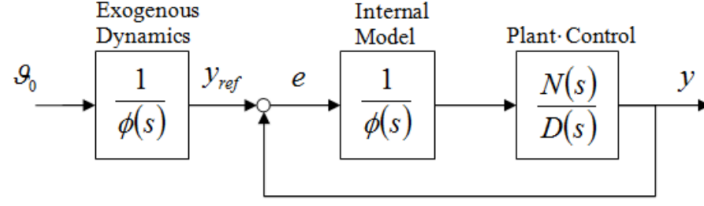


Fig. 2 The Internal Model Principle of Robust Regulation (Eqn. 8)

III. Motivating Example

A robust regulator (Sec. II.C) is designed for weaving target (Eqn. 1) intercepts. Then robust regulator and ProNav guidance miss distances against weaving targets are compared.

A. Robust Regulator & Weaving Target

As a motivating example, consider Eqn. 5 applied to the guidance loop Fig. 1. In four steps: 1) define the plant, 2) determine the exogenous dynamics, 3) define the regulated output, and 4) design the controller.

- 1) The single time constant autopilot response model has state space form, $A = 0$, $B = 1$, $C = 1$, $D = 0$. Time constant $\tau = 1$ is placed in Step 4.
- 2) Target maneuver, Eqn. 1, has state space form $\dot{\vartheta} = Z\vartheta$. Choose $\omega_T = 1$ (rad/sec) and $a_T = 1$ (g) with

$$Z = \begin{bmatrix} 0 & 1 \\ -\omega_T^2 & 0 \end{bmatrix}, \vartheta(0) = \begin{bmatrix} 0 \\ n_T \end{bmatrix} \quad (9)$$

- 3) Define the regulated output $e = n_T - n_C$. This is a simplification of ProNav Eqn. 3 which requires an integrator and the time varying gain $R_{GO} = V_C(t_F - t)$. The robust regulator replaces the forward path of Fig. 1.
- 4) Compute K to stabilize Eqn. 7 with $u = -K \begin{bmatrix} x \\ \eta \end{bmatrix}$. Choose poles $\{-1, -10 \pm 10i\}$. Time constant τ for plant state x is chosen in agreement with the ProNav guidance loop. Controller state η poles are computational, not physical, and can be faster.

The system Eqns. 5 with closed loop $u = -K \begin{bmatrix} x \\ \eta \end{bmatrix}$ is simulated and results plotted in Fig. 3. Each robust regulator is designed for a fixed ω_C , where $Z_c = \begin{bmatrix} 0 & 1 \\ -\omega_C^2 & 0 \end{bmatrix}$, the internal model of the exogenous dynamics, replaces Z in Eqn. 7. Fig. 3 shows robustness over a range of ω_T . Approximate knowledge of target maneuver period ω_C is the sole requirement for the internal model, robust regulator design.

B. Comparison

For consistent comparison of the ProNav guidance loop and robust regulator design above, choose the following:

- 1) Target maneuver Eqn. 1: $\omega_T = 1$ (rad/sec) and $a_T = 1$ (g)
- 2) Interceptor time constant τ in Fig 1: $\tau = 1$ (sec)
- 3) Guidance gain of Eqn. 2: $N' = 4$.

Application of guidance law Eqn. 2 to the ProNav loop Fig. 1 with target maneuver Eqn. 1 admits closed form solutions for peak steady state miss distance [2]. This peak miss distance normalized by maneuver magnitude a_T is the solid line plotted in Fig. 3 as a function of maneuver period ω_T . In general, ProNav peak steady state miss distance is most severe in the vicinity of $\omega_T \tau = 1$.

The dotted and dashed lines in Fig. 3 are normalized peak miss distance as a function of maneuver period ω_T for robust regulators designed for fixed estimates of maneuver period $\omega_C = \{1, 2\}$ (rad/sec) respectively. As shown in Fig. 3, performance is best at the design point. At the design point, $\omega_C = \omega_T$, performance is independent of a_T . Performance degradation is approximately linear in $\Delta\omega = \omega_T - \omega_C$. For fixed $\Delta\omega$, peak steady state miss distance is proportional to a_T . Fig. 3 shows robustness of two individual controllers; in addition, Fig. 3 implies selection from a small set of controllers may outperform ProNav guidance. Peak steady state miss distance is defined in Fig. 4 (a).

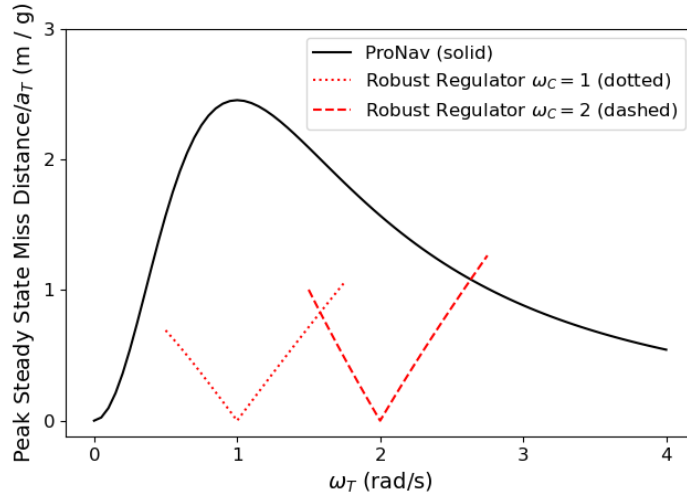


Fig. 3 Peak Steady State Miss Distance against Weaving Targets

IV. Autopilot as Robust Regulator

A robust regulator for a single time constant interceptor against a weaving target was designed in the previous section. This section implements robust regulation for a skid-to-turn interceptor against the same weaving target. A robust regulator is embedded into a skid-to-turn missile autopilot with aerodynamic control surfaces. The longitudinal axis autopilot computes a control, fin deflection δ , such that missile acceleration n_L responds to commanded acceleration n_c within performance specifications.

The normal acceleration generated by missile airframe angle of attack α and fin δ is

$$n_L \approx \dot{\gamma}V = V(Z_\alpha\alpha + Z_\delta\delta) \quad (10)$$

where

$$Z_\alpha = \frac{QS_{ref}}{m}C_{N\alpha}, \quad Z_\delta = \frac{QS_{ref}}{m}C_{N\delta}, \quad M_\alpha = \frac{QS_{ref}x_{ref}}{I_{yy}}C_{M\alpha}, \quad M_\delta = \frac{QS_{ref}x_{ref}}{I_{yy}}C_{M\delta}$$

The $C_{N\alpha}$, $C_{N\delta}$, $C_{M\alpha}$, $C_{M\delta}$ are the aerodynamic Normal force (C_N) & Moment (C_M) coefficient derivatives with respect to α and δ . See for example [1]. The airframe equations of motion are found by substituting $\alpha = \theta - \gamma$ into Eqn. 10 and also summing moments to obtain

$$\dot{\alpha} = -Z_\alpha\alpha + q + -Z_\delta\delta \quad (11)$$

$$\dot{q} = M_\alpha\alpha + M_\delta\delta \quad (12)$$

where $\ddot{\theta} \equiv \dot{q}$. The autopilot equations of motion in state space form (Eqn. 4) are

$$A = \begin{bmatrix} -Z_\alpha & 1 \\ M_\alpha & 0 \end{bmatrix}, \quad B = \begin{bmatrix} -Z_\delta \\ M_\delta \end{bmatrix}, \quad C = \begin{bmatrix} Z_\alpha V & 0 \end{bmatrix}, \quad D = [Z_\delta V] \quad (13)$$

with state vector $x^T = \begin{bmatrix} \alpha & q \end{bmatrix}^T$.

Embed Eqn. 13 into Eqn. 7 to complete the robust regulator autopilot controller. For Eqn. 6, choose $J = \begin{bmatrix} 0 \\ 1 \end{bmatrix}$.

Controller synthesis Eqn. 7 is

$$\begin{bmatrix} \dot{\alpha} \\ \dot{q} \\ \dot{\eta}_1 \\ \dot{\eta}_2 \end{bmatrix} = \begin{bmatrix} -Z_\alpha & 1 & 0 & 0 \\ M_\alpha & 0 & 0 & 0 \\ Z_\alpha V & 0 & 0 & 1 \\ 0 & 0 & -\omega_C^2 & 0 \end{bmatrix} \begin{bmatrix} \alpha \\ q \\ \eta_1 \\ \eta_2 \end{bmatrix} + \begin{bmatrix} -Z_\delta \\ M_\delta \\ Z_\delta V \\ 0 \end{bmatrix} u \quad (14)$$

Two controllers are designed identical except for assumed target weave frequency ω_C :

- 1) Choose autopilot aerodynamic coefficients, approximating [1] Chapter 22,

$$\{Z_\alpha, Z_\delta, M_\alpha, M_\delta\} = \{3, 0.5, -500., -600.\} \quad (15)$$

- 2) Choose controller internal model of the weave frequency at $\omega_C = \{3, 5\}$ (rad/s),
- 3) Choose controller poles $\{-3, -4, -35 \pm 35i\}$.

Then use a pole placement algorithm to obtain K such that the poles of Eqn. 14 with $u = -Kx$ match Step 3. The application of these two controllers to maneuvering threat (Eqn. 1) over a range of weave frequencies ω_T is shown in Fig. 4 (b). Both controllers have an error of less than 1 (m/g) when $|\omega_C - \omega_T| \approx 1$ (rad/s). However, the ProNav guidance loop of Figure 1 with time constant $\tau = \frac{1}{3}$ (s) has an error of approximately 2.5 (m/g) at $\omega_T = 3$ (rad/s). Also, the robust regulator is insensitive to modest variation in the plant parameters (e.g. aerodynamic coefficients).

Define a closed loop state vector with autopilot plant x , error driven controller η , and exogenous dynamic states ϑ as

$$x_{CL} = \begin{bmatrix} x & \eta & \vartheta \end{bmatrix}^T$$

Obtain the closed loop, LTI system equations of motion by appending the exogenous dynamics $\dot{\vartheta} = Z\vartheta$ to Eqn. 7. Choose initial conditions

$$x(0) = \begin{bmatrix} 0 & 0 & 0 & 0 & 0 & 9.81 \end{bmatrix}^T$$

The time response is plotted in Fig 4 (a). The error dynamic system states η are not initialized to the exogenous dynamic states ϑ . Recall the error Eqn. 5 is $e = y_{ref} - y = F\vartheta - (Cx + Du)$. After a short transient period, the steady state error is sinusoidal; the amplitude of the error sine wave is the peak steady state error.

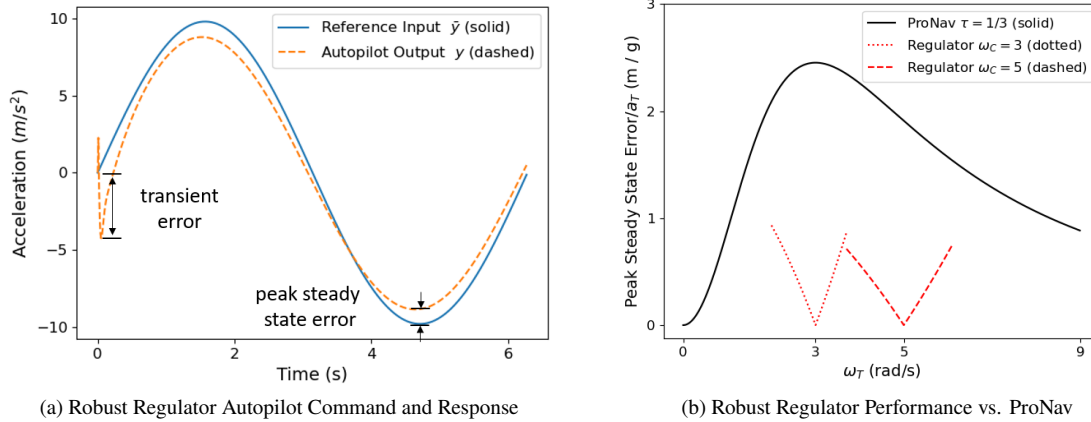


Fig. 4 Embedded Autopilot Robust Regulator

Remark: Instead of sinusoidal threat maneuvers, let Eqn. 1 be a step acceleration maneuver $a_T u(t)$ where $u(t)$ has Laplace transform $\frac{1}{s}$. The error driven controller Eqn. 6 is now $J = 1, Z = 0$, i.e. an integrator. Then Eqn. 7 with an integrator (instead of oscillator Eqn. 9) can be shown equivalent to the “three loop Nesline” autopilot [6] via similarity transformation.

V. Conclusion

Robust regulation for weaving targets as an alternative to proportional navigation guidance is demonstrated. Either one regulator with on-line adjustment or a small set of pre-designed regulators may provide superior miss distance. Future work involves 1) remove the simplification in Step 3 of Sec. III.A, e.g. include a time (or range) varying gain, and 2) applications with realistic geometry, state estimation, and controller selection.

References

- [1] Zarchan, P., *Tactical and Strategic Missile Guidance*, Vol. 176, Progress in Astronautics and Aeronautics, AIAA, 1997.
- [2] Zarchan, P., "Proportional Navigation and Weaving Targets," *Journal of Guidance, Control and Dynamics*, Vol. 18, No. 5, 1995, pp. 969–974.
- [3] Kwatny, H. G., and Kalnitsky, K. C., "On Alternative Methodologies for the Design of Robust Linear Multivariable Regulators," *IEEE Transactions on Automatic Control*, Vol. AC-23, No. 5, 1978, pp. 930–933.
- [4] Francis, B. A., and Wonham, W. M., "The Internal Model Principle for Linear Multivariable Regulators," *Applied Mathematics and Optimization*, Vol. 2, 1975, pp. 170–194.
- [5] Chen, C. T., *Linear System Theory and Design*, Oxford University Press, New York, 1984.
- [6] Nesline, F. W., and Nesline, M. L., "How autopilot requirements constrain the aerodynamic design of homing missiles," *American Control Conference*, IEEE, 1984, pp. 716–730.
- [7] Berg, J., and Kwatny, H. G., "An Upper Bound on the Structurally Stable Regulation of a Parameterized Family of Nonlinear Control Systems," *Systems and Control Letters*, Vol. 23, 1994, pp. 85–95.